

4-1-2015

# Revisiting the Renner–Teller Effect in the $X^-{}^2\Pi$ State of CCN: Pulsed Discharge-supersonic Jet Single Vibronic Level Emission Spectroscopy

Lloyd Godfrey Muzangwa

*Marquette University*

Scott Reid

*Marquette University*, scott.reid@marquette.edu

Marquette University

e-Publications@Marquette

**Department of Chemistry Faculty Research and Publications/College of Arts and Sciences**

**This paper is NOT THE PUBLISHED VERSION; but the author's final, peer-reviewed manuscript.** The published version may be accessed by following the link in the citation below.

*Journal of Molecular Spectroscopy*, Vol. 310 (April 2015): 105-108. [DOI](#). This article is © Elsevier and permission has been granted for this version to appear in [e-Publications@Marquette](#). Elsevier does not grant permission for this article to be further copied/distributed or hosted elsewhere without the express permission from Elsevier.

## Revisiting the Renner–Teller effect in the $\tilde{X}^2\Pi$ state of CCN: Pulsed discharge-supersonic jet single vibronic level emission spectroscopy

Lloyd Muzangwa

Department of Chemistry, Marquette University, Milwaukee, WI

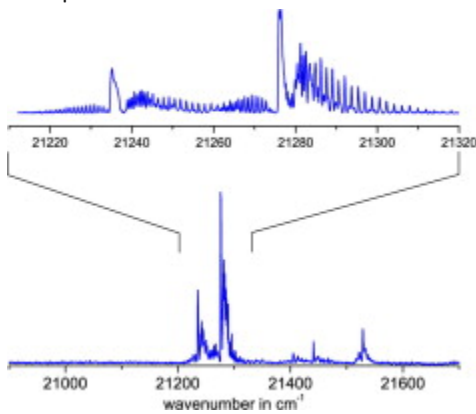
Scott A. Reid

Department of Chemistry, Marquette University, Milwaukee, WI

### Abstract

The CCN radical is a prototypical system for study of the Renner–Teller effect in its degenerate  $\tilde{X}^2\Pi$  ground state, with a number of experimental and theoretical studies carried out over the past 50 years. Most experimental studies have focused on the low-lying vibrational structure as observed in the high-resolution spectra of hot bands, or in emission. In this work, we have used pulsed-discharge supersonic-jet single vibronic level (SVL) emission spectroscopy from selected levels of the  $\tilde{A}^2\Delta$  state to probe the vibronic structure of  $\tilde{X}^2\Pi$  up to  $\sim 6000 \text{ cm}^{-1}$  above the vibrationless level. Around 50 levels were assigned, and these were fit to a Renner–Teller Hamiltonian to derive a detailed set of spectroscopic constants. Our data are compared with the results of recent high level coupled cluster calculations.

## Graphical abstract



## Keywords

CCN radical, Carbene, Renner–Teller effect, Emission spectroscopy

## 1. Introduction

The CCN radical is a prototypical free radical of the C<sub>x</sub>N family, and is thought to be an important intermediate in the interstellar medium, although its small dipole moment has to date hampered its detection by radioastronomy.<sup>1</sup> It is also a prototypical system for study of the Renner–Teller effect, a coupling of vibrational and electronic angular momentum in orbitally degenerate states. The initial observation of the UV–Visible spectrum of CCN was found in the flash photolysis studies of Merer and Travis in 1965,<sup>2</sup> which characterized three band systems ( $\tilde{X}^2\Pi - \tilde{A}^2\Delta$ ,  $\tilde{X}^2\Pi - \tilde{B}^2\Sigma^-$ ,  $\tilde{X}^2\Pi - \tilde{C}^2\Sigma^+$ ) and the RT effect in the  $\tilde{X}^2\Pi$  and  $\tilde{A}^2\Delta$  states. Since then, numerous experimental studies have examined the spectroscopy of this radical. These include Laser Induced Fluorescence (LIF) excitation and emission in the gas phase and solid Ar,<sup>3–9</sup> microwave-optical double resonance,<sup>10</sup> Fourier Transform emission,<sup>11,12</sup> Fourier transform microwave,<sup>13</sup> infrared,<sup>14,15</sup> laser magnetic resonance,<sup>16,17</sup> and photoelectron spectroscopy.<sup>18</sup>

The experimental studies to date have provided detailed, if incomplete, information on the Renner–Teller effect in the ground  $\tilde{X}^2\Pi$  state. Thus, for example, Hakuta and Uehara exploited a resonance of the CCN spectrum with the blue-green Ar<sup>+</sup> laser line to obtain emission spectra for the  $\tilde{A}^2\Delta:(0, 1, 0)\Phi - \tilde{X}^2\Pi:(0, \nu_2, \nu_3)\Delta$  transitions, and also observed the collision-induced  $\tilde{A}^2\Delta:(0, 1, 0)\Pi - \tilde{X}^2\Pi:(\nu_1, 1, \nu_3)\Sigma^+, \Sigma^-$  transitions. Building upon these studies, Bernath and co-workers used Fourier Transform emission spectroscopy to derive rotational constants for several vibronic levels of the ground state in the (0,  $\nu_2$ , 1) and ( $\nu_1$ , 0,  $\nu_3$ ) manifolds.<sup>11,12</sup> Hirota and co-workers used high resolution laser spectroscopy to probe the origin band and two hot bands of the  $\tilde{X}^2\Pi - \tilde{A}^2\Delta$  system, yielding information on the rotational and fine-structure constants of the two electronic states.<sup>5,10</sup> Subsequently, Endo and co-workers probed the spectroscopy of the  $\tilde{X}^2\Pi - \tilde{C}^2\Sigma^+$  transition under jet-cooled conditions using LIF, which gave new information on the level structure of the  $\tilde{X}^2\Pi$  state.<sup>9</sup> More detailed information on the low-lying bending levels of this state was provided in the laser magnetic resonance experiments of Evenson, Brown and co-workers.<sup>17</sup>

The experimental studies of CCN have been complemented from the very beginning by computational investigation of the electronic structure of this radical.<sup>19</sup> These studies were also motivated in part by the desire

to identify CCN in the interstellar medium [1]. In 1994, Rosmus and co-workers calculated the rovibronic levels of the  $\tilde{X}^2\Pi$  state using Complete Active Space Self-consistent Field (CASSCF) methods,<sup>20</sup> which reproduced the experimentally known levels with an accuracy of  $\sim 10\text{--}20 \text{ cm}^{-1}$ . Around the same time, Gijbels and co-workers reported CASSCF, multireference Configuration Interaction (MRCI), and coupled cluster calculations on the structure and electronic states of CCN.<sup>21</sup> Over the past decade, other computational studies have appeared.<sup>22-28</sup> Of most relevance to this work are the very recent calculations by Peterson and co-workers of the ro-vibronic level structure of the ground state of CCN using explicitly correlated methods, which reported vibronic energies for levels up to  $\sim 3000 \text{ cm}^{-1}$  above the vibrationless level.<sup>29</sup>

In this work we have used Single Vibronic Level (SVL) emission spectroscopy from selected vibrational levels of the  $\tilde{A}^2\Delta$  state, in concert with pulsed-jet discharge techniques, to probe the vibronic level structure of the  $\tilde{X}^2\Pi$  state up to an energy of  $\sim 6000 \text{ cm}^{-1}$  above the vibrationless level. In beginning this work, we were motivated by the recent *ab initio* studies, and by the fact that no global investigation of the level structure of the  $\tilde{X}^2\Pi$  state has to date been performed. In comparison with previous work, our study provides a lower resolution but more comprehensive view of the level structure. A global fit of our data is reported, and we compare our results with the recent high level *ab initio* calculations of Peterson and co-workers.<sup>29</sup>

## 2. Experimental and computational methods

The experimental apparatus for LIF and SVL emission studies used in this work has previously been described in detail.<sup>30-52</sup> Briefly, CCN was generated by a pulsed electrical discharge through a mixture of CH<sub>3</sub>CN in Ar, obtained by passing high purity Ar gas at a pressure of  $\sim 2$  bar through a stainless steel bubbler containing the chemical. The bubbler was placed in a refrigerated bath that was typically held at  $-5^\circ\text{C}$ . Discharge was initiated by a  $+1000 \text{ V}$  pulse of  $50 \mu\text{s}$  duration, through a current limiting ballast resistor. The timing of laser, nozzle, and discharge firing was controlled by an eight channel digital delay generator (Berkeley Nucleonics model 565), which also generated a variable width gate pulse for the high voltage pulser.

The laser system used in this work consisted of a tunable dye laser (Lambda-Physik Scanmate 2E) pumped by the third harmonic of a Nd:YAG laser (Continuum NY-61). The laser beam was not focused, and typical pulse energies were  $\sim 1\text{--}2 \text{ mJ}$  in a  $\sim 3 \text{ mm}$  diameter beam. A portion of the dye laser fundamental was sent into a Fe–Ne or Fe–Ar lamp for absolute wavelength calibration using the optogalvanic effect. These measurements utilized a mutually orthogonal geometry of laser, molecular beam, and detector, where the laser beam crossed the molecular beam at a distance of  $\sim 15 \text{ mm}$  (19 nozzle diameters) downstream. Fluorescence was collected and collimated by a f/2.4 plano-convex lens, and focused using a second 2 in dia. f/3.0 lens either: (a) through a long-pass cutoff filter onto a photomultiplier tube detector (PMT, Oriel 77348) for monitoring total fluorescence, or (b) onto the slit of a 0.3 m spectrograph (ANDOR Schamrock) equipped with a gated intensified charge coupled device detector (ICCD; ANDOR Istar) for wavelength resolved emission spectra. Typical slit widths were 0.10–0.25 mm, and lower and higher resolution spectra were obtained, respectively, with 600 l/mm and 1800 l/mm gratings. Spectra were typically accumulated over 10 000 laser shots. Background spectra were also obtained with the laser blocked to identify emission lines from the discharge. The spectrograph was calibrated using emission lines from a Fe:Ne hollow cathode lamp.

Fluorescence excitation spectra were acquired by integrating the PMT output using a gated integrator (Stanford Research SR250). The integrator output was digitized by a 12 bit analog to digital converter (Measurement

Computing USB-1208FS), and passed to a computer for analysis. Data collection and laser wavelength control was achieved using LABVIEW software.

### 3. Results and discussion

[Fig. 1](#) shows a survey fluorescence excitation spectrum (lower panel) of the CCN radical in the region of the origin band of the  $\tilde{X}^2\Pi - \tilde{A}^2\Delta$  system. A higher resolution spectrum of the origin band is shown at top in this figure; note that Hirota and co-workers previously examined this band at very high resolution using microwave-optical double resonance spectroscopy.<sup>10</sup> Our focus in this work is the vibronic structure of the  $\tilde{X}^2\Pi$  state, and to that end we measured SVL emission spectra from several bands in this spectrum (noted with arrows), which included both spin-orbit components of the origin band and also the  $\tilde{X}^2\Pi(0,1,0)\Sigma^- - \tilde{A}^2\Delta(0,1,0)\Pi$  hot band centered at  $21527.5\text{ cm}^{-1}$ .

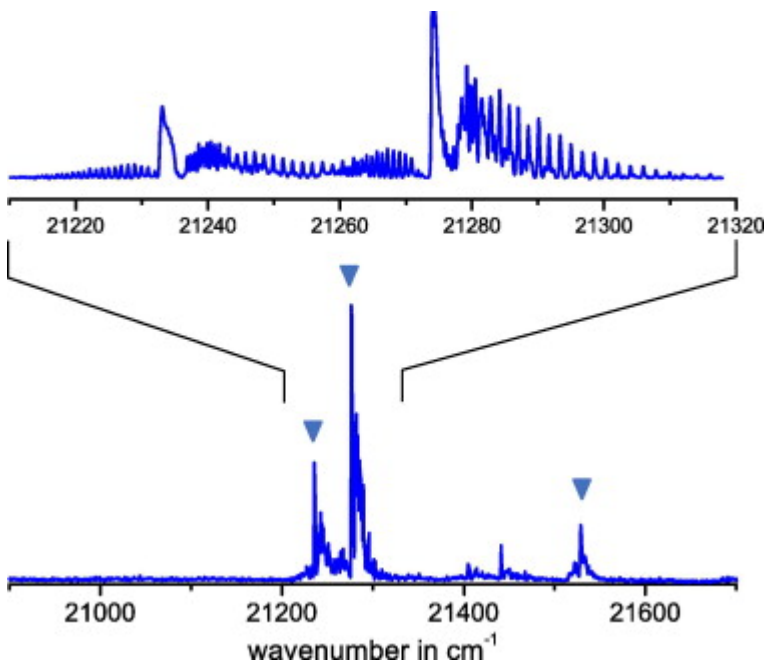


Fig. 1. *Lower panel:* Survey fluorescence excitation spectra of the CCN radical in the region of the origin transition of the  $X\sim 2\Pi$ - $A\sim 2\Delta$  system. *Upper panel:* Expanded view of the origin band.

Representative SVL emission spectra obtained following excitation of the  $\tilde{X}^2\Pi_{1/2}(0,0,0) - \tilde{A}^2\Delta(0,0,0)$  sub-band are shown in [Fig. 2](#). The lower panel displays a survey spectrum obtained with at lower resolution (600 l/mm grating), while the upper panel displays a portion of the same region measured at higher resolution (1800 l/mm grating). The dominant transitions terminate in lower state levels with  $\Pi$  symmetry, and prominent progressions involving both stretching vibrations are observed, as noted. In contrast, spectra obtained following excitation of the  $\tilde{X}^2\Pi(0,1,0)\Sigma^- - \tilde{A}^2\Delta(0,1,0)\Pi$  transition afforded access to ground state levels of  $\Sigma$  symmetry. Overall, nearly 50 levels in the ground state were assigned and fit.

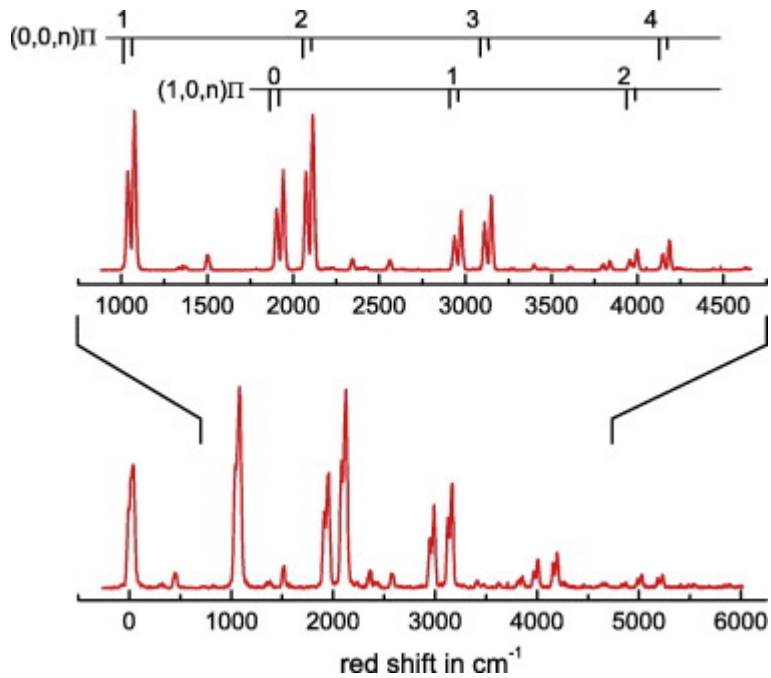


Fig. 2. *Lower Panel:* Survey Single Vibronic Level (SVL) emission spectrum from the origin band of the  $X \sim 2\Pi$ - $A \sim 2\Delta$  system. *Upper panel:* SVL emission spectra obtained at higher resolution. Assignments of the most prominent features are included.

The term energies derived from our emission spectra were used to conduct a global analysis of the vibronic level structure in the  $\tilde{X}^2\Pi$  state. The data were fit to an effective Renner-Teller Hamiltonian for a  ${}^2\Pi$  state using the RT3 program recently developed by He and Clouthier.<sup>53</sup> The fit residual was  $2.3\text{ cm}^{-1}$ , which is similar to our experimental uncertainty of  $2.0\text{ cm}^{-1}$ . The observed level positions, assignments, and fit residuals are given in Table 1, while Table 2 lists the derived fit parameters. In the fit the parameters  $\varepsilon\omega$ , the Renner parameter, and  $g_k$ , which describes the  $K$  dependent vibronic mixing, were fixed at the previously determined values.<sup>17</sup> The constants that account for the variation of the spin-orbit parameter with vibrational level ( $\alpha_i$ ) were small and not well determined by our data – these were thus fixed to 0 in the fit. Note that the calculated values of these constants are on the order of  $0.003\text{ cm}^{-1}$ .<sup>29</sup>

Table 1. Comparison of observed, fit and calculated (from Ref. 29) line positions in the  $X^2\Pi$  state of the CCN radical.

Energy	$P$	Assignment	Fit	Obs-Fit	Calc (Ref. 29)	Obs-Cal
38.9	1.5	$\kappa(0, 0, 0) \Pi$	39.7	-0.7	38.9	0.1
199.0	0.5	$\mu(0, 1, 0) \Sigma$	201.9	-2.9	201.0	-2.0
295.0	1.5	$\mu(0, 1, 0) \Delta$	295.7	-0.3	295.3	0.1
476.0	0.5	$\kappa(0, 1, 0) \Sigma$	476.8	-0.7	478.8	-2.7
579.0	2.5	$\mu(0, 2, 0) \Phi$	581.1	-1.7	580.3	-0.9
1051.0	0.5	$\mu(0, 0, 1) \Pi$	1046.2	5.2	1052.0	-1.0

Energy	$P$	Assignment	Fit	Obs–Fit	Calc (Ref. <a href="#">29</a> )	Obs–Cal
1089.0	1.5	$\kappa(0, 0, 1) \Pi$	1086.0	3.0	1090.8	-1.8
1253.0	0.5	$\mu(0, 1, 1) \Sigma$	1249.6	3.4	1263.5	-10.5
1253.0	0.5	$\kappa(0, 3, 0) \Sigma$	1252.6	0.4	1236.6	16.4
1349.0	1.5	$\mu(0, 1, 1) \Delta$	1343.6	5.4	1357.4	-8.4
1383.0	2.5	$\kappa(0, 1, 1) \Delta$	1379.5	3.5	1391.7	-8.7
1523.0	0.5	$\mu(0, 1, 1) \Sigma$	1524.5	-1.5	...	...
1756.0	0.5	$\mu(0, 3, 1) \Sigma$	1757.1	-1.2	1767.1	-11.1
1915.3	0.5	$\mu(1, 0, 0) \Pi$	1915.1	0.2	1924.9	-9.6
1954.2	1.5	$\kappa(1, 0, 0) \Pi$	1954.8	-0.6	1963.6	-9.4
2086.6	0.5	$\mu(0, 0, 2) \Pi$	2088.1	-1.5	2097.4	-10.8
2107.5	0.5	$\mu(1, 1, 0) \Sigma$	2109.2	-1.7	2117.5	-10.0
2125.7	1.5	$\kappa(0, 0, 2) \Pi$	2127.9	-2.2	2136.0	-10.3
2204.7	1.5	$\mu(1, 1, 0) \Delta$	2202.4	2.3	2212.9	-8.2
2238.9	2.5	$\kappa(1, 1, 0) \Delta$	2237.9	1.0	2247.7	-8.8
2304.2	0.5	$\kappa(0, 3, 1) \Sigma$	2303.7	0.5	2298.7	6.5
2383.7	0.5	$\kappa(1, 1, 0) \Sigma$	2384.3	-0.6	2395.3	-12.4
2565.5	0.5	$\kappa(0, 1, 2) \Sigma$	2567.9	-2.4	2578.1	-12.6
2949.1	0.5	$\mu(1, 0, 1) \Pi$	2946.6	2.5	...	...
2987.1	1.5	$\kappa(1, 0, 1) \Pi$	2986.2	0.9	...	...
3124.2	0.5	$\mu(0, 0, 3) \Pi$	3125.6	-1.4	...	...
3163.2	1.5	$\kappa(0, 0, 3) \Pi$	3165.4	-2.2	...	...
3350.9	0.5	$\kappa(0, 3, 2) \Sigma$	3350.5	0.4	...	...
3419.9	0.5	$\kappa(1, 1, 1) \Sigma$	3417.2	2.7	...	...
3604.5	0.5	$\kappa(0, 1, 3) \Sigma$	3606.8	-2.3	...	...
3811.8	0.5	$\mu(2, 0, 0) \Pi$	3812.0	-0.2	...	...
3851.3	1.5	$\kappa(2, 0, 0) \Pi$	3851.5	-0.2	...	...
3970.2	0.5	$\mu(1, 0, 2) \Pi$	3973.6	-3.4	...	...
3998.1	0.5	$\mu(2, 1, 0) \Sigma$	3998.2	-0.1	...	...
4009.8	1.5	$\kappa(1, 0, 2) \Pi$	4013.3	-3.5	...	...

Energy	<i>P</i>	Assignment	Fit	Obs–Fit	Calc (Ref. 29)	Obs–Cal
4159.9	0.5	$\mu(0, 0, 4) \Pi$	4158.7	1.2	...	...
4198.7	1.5	$\kappa(0, 0, 4) \Pi$	4198.5	0.2	...	...
4271.5	0.5	$\kappa(2, 1, 0) \Sigma$	4273.5	-2.0	...	...
4445.9	0.5	$\kappa(1, 1, 2) \Sigma$	4445.7	0.2	...	...
4640.7	0.5	$\kappa(0, 1, 4) \Sigma$	4641.5	-0.8	...	...
4829.7	0.5	$\mu(2, 0, 1) \Pi$	4828.7	1.0	...	...
4870.1	1.5	$\kappa(2, 0, 1) \Pi$	4868.1	2.0	...	...
5188.9	0.5	$\mu(0, 0, 5) \Pi$	5187.5	1.4	...	...
5231.0	1.5	$\kappa(0, 0, 5) \Pi$	5227.3	3.7	...	...
5838.1	0.5	$\mu(2, 0, 2) \Pi$	5840.9	-2.8	...	...
5885.4	1.5	$\kappa(2, 0, 2) \Pi$	5880.4	5.0	...	...
			SD	2.3		7.1

Table 2. Fit parameters for the  $X^2\Pi$  state of the CCN radical.

Parameter	Fit value	Calc. (Ref. 29)
$\omega_1$	1924.7(19)	1967.2
$\omega_2$	317.7(17)	322.2
$\omega_3$	1048.3(9)	1058.3
$\varepsilon\omega$	133.639 <sup>a</sup>	138.1
$g_k$	2.5 <sup>a</sup>	...
$A$	41.8(10)	...
$g_4$	1.0(3)	...
$g^4$	0.3(1)	...
$x_{11}$	-9.1(9)	-13.3
$x_{12}$	-7.7(11)	-7.9
$x_{13}$	-14.8(7)	-19.1
$x_{23}$	1.5(4)	7.0
$x_{33}$	-2.2(2)	-2.6

<sup>a</sup>Values constrained to those previously determined – see text for details.

While the data reported here are of low resolution compared to some of the earlier studies, they extend over a much broader energy range, and thus we have derived an improved set of anharmonicity parameters (Table 2).

These are largely in good agreement with theoretical expectations, with the positive anharmonicity predicted for  $x_{23}$  reproduced.<sup>29</sup> The measured term energies are in good agreement with the values calculated by Peterson and co-workers, displaying a standard deviation of  $7.4\text{ cm}^{-1}$  over the comparison set of 20 levels (Table 2). This illustrates the power of explicitly correlated methods for reproducing the rovibronic level structure of open shell systems such as the CCN radical.

A complication that often arises in the spectra of triatomic molecules is the presence of Fermi-resonance interactions between a stretching vibration and the bending mode. However, in this work there is no evidence of a strong stretch-bend interaction, as including such an interaction did not improve the overall fit quality.

## 4. Conclusions

In this work we have examined the vibronic level structure of the  $\tilde{X}^2\Pi$  ground state of the CCN radical using pulsed discharge methods in combination with single vibronic level emission spectroscopy. By exploiting transitions from single vibronic levels in the  $\tilde{A}^2\Delta$  state of this radical, transitions to more than 50 ground state vibronic levels were observed. The resulting data afford a global view of the Renner–Teller interaction in the ground state, and a fit of the data has yielded an improved set of anharmonicity constants. Our data are in good agreement with the predictions of recent high level *ab initio* predictions using explicitly correlated methods, which reproduce the observed level structure with a standard deviation of  $\sim 7\text{ cm}^{-1}$ .

## Acknowledgments

Support of the research by the National Science Foundation (CHE-1057951) is gratefully acknowledged. The authors thank Silver Nyambo for experimental assistance.

## References

- <sup>1</sup>G.W. Fuchs, U. Fuchs, T.F. Giesen, F. Wyrowski. *Astron. Astrophys.*, 426 (2004), pp. 517-521
- <sup>2</sup>A.J. Merer, D.N. Travis. *Can. J. Phys.*, 43 (1965), pp. 1795-1830
- <sup>3</sup>V.E. Bondybey, J.H. English. *J. Mol. Spectrosc.*, 70 (1978), pp. 236-242
- <sup>4</sup>W. Weltner Jr., D. McLeod Jr. *J. Chem. Phys.*, 45 (1966), pp. 3096-3105
- <sup>5</sup>K. Kawaguchi, T. Suzuki, S. Saito, E. Hirota, T. Kasuya. *J. Mol. Spectrosc.*, 106 (1984), pp. 320-329
- <sup>6</sup>K. Kawaguchi, T. Suzuki, K. Hakuta, E. Hirota, T. Kasuya. *Reza Kagaku Kenkyu*, 5 (1983), pp. 22-25
- <sup>7</sup>K. Hakuta, H. Uehara. *J. Chem. Phys.*, 78 (1983), pp. 6484-6489
- <sup>8</sup>K. Kawaguchi, T. Suzuki, S. Saito, E. Hirota, T. Kasuya. *Reza Kagaku Kenkyu*, 4 (1982), pp. 19-25
- <sup>9</sup>H. Kohguchi, Y. Ohshima, Y. Endo. *J. Chem. Phys.*, 106 (1997), pp. 5429-5438
- <sup>10</sup>T. Suzuki, S. Saito, E. Hirota. *J. Chem. Phys.*, 83 (1985), pp. 6154-6157
- <sup>11</sup>C.R. Brazier, L.C. O'Brien, P.F. Bernath. *J. Chem. Phys.*, 86 (1987), pp. 3078-3081
- <sup>12</sup>N. Oliphant, A. Lee, P.F. Bernath, C.R. Brazier. *J. Chem. Phys.*, 92 (1990), pp. 2244-2247
- <sup>13</sup>Y. Ohshima, Y. Endo. *J. Mol. Spectrosc.*, 172 (1995), pp. 225-232
- <sup>14</sup>M. Feher, C. Salud, J.P. Maier. *J. Mol. Spectrosc.*, 145 (1991), pp. 246-250
- <sup>15</sup>S.A. Beaton, D.A. Gillett, J.M. Brown, M. Feher, A. Rohrbacher. *J. Mol. Spectrosc.*, 209 (2001), pp. 60-65
- <sup>16</sup>D.A. Gillett, J.M. Brown. *Can. J. Phys.*, 72 (1994), pp. 1001-1006
- <sup>17</sup>M.D. Allen, K.M. Evenson, D.A. Gillett, J.M. Brown. *J. Mol. Spectrosc.*, 201 (2000), pp. 18-29
- <sup>18</sup>E. Garand, T.I. Yacovitch, D.M. Neumark. *J. Chem. Phys.*, 130 (2009), pp. 064304/1-064304/7
- <sup>19</sup>S. Green. *Astrophys. J.*, 240 (1980), pp. 962-967
- <sup>20</sup>W. Gabriel, E.A. Reinsch, P. Rosmus. *Chem. Phys. Lett.*, 231 (1994), pp. 13-17
- <sup>21</sup>J.M.L. Martin, P.R. Taylor, J.P. Francois, R. Gijbels. *Chem. Phys. Lett.*, 226 (1994), pp. 475-483

- [22R. Prasad, P. Chandra. Indian J. Chem., Sect. A: Inorg., Bio-inorg., Phys., Theor. Anal. Chem., 39A \(2000\), pp. 148-162](#)
- [23J.J. Belbruno, Z.-C. Tang, R. Smith, S. Hobday. Mol. Phys., 99 \(2001\), pp. 957-967](#)
- [24R. Prasad, P. Chandra. J. Chem. Phys., 114 \(2001\), pp. 1589-1600](#)
- [25G.W. Fuchs, U. Fuchs, T.F. Giesen, G. Winnewisser, F. Wyrowski, M.C. McCarthy, C.A. Gottlieb, J. Kucera, P. Thaddeus. Springer Proc. Phys., 91 \(2004\), pp. 99-102](#)
- [26J. Wang, Y.-H. Ding, C.-C. Sun. ChemPhysChem, 7 \(2006\), pp. 710-722](#)
- [27M. Ehara, J.R. Gour, P. Piecuch. Mol. Phys., 107 \(2009\), pp. 871-880](#)
- [28A.M. Mebel, R.I. Kaiser. Astrophys. J., 564 \(2002\), pp. 787-791](#)
- [29H.J. Grant, A. Mitrushchenkov, K.E. Yousaf, K.A. Peterson. J. Chem. Phys., 135 \(2011\), p. 144309/12](#)
- [30H. Fan, I. Ionescu, C. Annesley, S.A. Reid. Chem. Phys. Lett., 378 \(2003\), pp. 548-552](#)
- [31H. Fan, I. Ionescu, C. Annesley, J. Cummins, M. Bowers, S.A. Reid. J. Mol. Spectr., 225 \(2004\), pp. 43-47](#)
- [32I. Ionescu, H. Fan, C. Annesley, J. Xin, S.A. Reid. J. Chem. Phys., 120 \(2004\), pp. 1164-1167](#)
- [33H. Fan, I. Ionescu, J. Xin, S.A. Reid. J. Chem. Phys., 121 \(2004\), pp. 8869-8873](#)
- [34I. Ionescu, H. Fan, E. Ionescu, S.A. Reid. J. Chem. Phys., 121 \(2004\), pp. 8874-8879](#)
- [35H. Fan, I. Ionescu, C. Annesley, J. Cummins, M. Bowers, J. Xin, S.A. Reid. J. Phys. Chem. A, 108 \(2004\), pp. 3732-3738](#)
- [36H. Fan, C. Mukarakate, M. Deselnicu, C. Tao, S.A. Reid. J. Chem. Phys., 123 \(2005\), p. 014314/7](#)
- [37E. Ionescu, S.A. Reid. J. Mol. Struct. THEOCHEM, 725 \(2005\), pp. 45-53](#)
- [38C. Mukarakate, Y. Mishchenko, D. Brusse, C. Tao, S.A. Reid. Phys. Chem. Chem. Phys., 8 \(2006\), pp. 4320-4326](#)
- [39M. Deselnicu, C. Tao, C. Mukarakate, S.A. Reid. J. Chem. Phys., 124 \(2006\). 134302/11](#)
- [40C. Tao, M. Deselnicu, C. Mukarakate, S.A. Reid. J. Chem. Phys., 125 \(2006\). 094305/9](#)
- [41C. Tao, C. Mukarakate, S.A. Reid. J. Chem. Phys., 124 \(2006\). 224314/11](#)
- [42C. Tao, M. Deselnicu, H. Fan, C. Mukarakate, I. Ionescu, S.A. Reid. Phys. Chem. Chem. Phys., 8 \(2006\), pp. 707-713](#)
- [43C. Tao, C. Mukarakate, S.A. Reid. J. Mol. Spectr., 241 \(2007\), pp. 136-142](#)
- [44C. Tao, C. Mukarakate, D. Brusse, Y. Mishchenko, S.A. Reid. J. Mol. Spectr., 241 \(2007\), pp. 180-185](#)
- [45C. Tao, C. Mukarakate, S.A. Reid. J. Mol. Spectr., 246 \(2007\), pp. 113-117](#)
- [46C. Tao, C. Mukarakate, S.A. Reid. J. Mol. Spectr., 241 \(2007\), pp. 143-150](#)
- [47C. Tao, S.A. Reid, T.W. Schmidt, S.H. Kable. J. Chem. Phys., 126 \(2007\). 051105/4](#)
- [48C.A. Richmond, C. Tao, C. Mukarakate, H. Fan, K. Nauta, T.W. Schmidt, S.H. Kable, S.A. Reid. J. Phys. Chem. A, 112 \(2008\), pp. 11355-11362](#)
- [49C. Tao, C. Mukarakate, R.H. Judge, S.A. Reid. J. Chem. Phys., 128 \(2008\), p. 171101/4](#)
- [50C. Tao, C. Mukarakate, Z. Terranova, C. Ebban, R.H. Judge, S.A. Reid. J. Chem. Phys., 129 \(2008\). 104309/8](#)
- [51C. Mukarakate, C. Tao, C.D. Jordan, W.F. Polik, S.A. Reid. J. Phys. Chem. A, 112 \(2008\), pp. 466-471](#)
- [52C. Tao, C. Ebban, H.-T. Ko, S.A. Reid. Phys. Chem. Chem. Phys., 10 \(2008\), pp. 6090-6092](#)
- [53S.G. He, D.J. Clouthier. Comput. Phys. Commun., 178 \(2008\), pp. 676-684](#)